

of SAH are drying and heating for agriculture and industrial applications, marine products, environment heating, and air-conditioning systems, see [Yadav \(2015\)](#). Thermal performance for conventional SAH system (with smooth heated absorber plate) is generally poor and the heat transfer coefficient is low due to the creation of viscous sub-layer at the solar air heater absorber plate. The flow turbulence must be enhanced in the absorber plate to disturb the viscous sub-layer and motivate the creation many reattachment zones by the insertion of artificial surface roughness. The inserted ribs should have a relatively small height compared to the duct dimensions for less energy consumption, see [Jaurker *et al.* \(2006\)](#). The disturbed viscous sub-layer for the improvement in heat transfer using artificial surface roughness induces relatively higher pressure drop of the flowing fluid flow. However, the presence of artificially roughness along the heated absorber plate is shown to be substantially thermally efficient compared to the conventional SAH. [Yadav and Bhagoria \(2013b, 2014a and 2014b\)](#) performed numerical analysis with different artificial surface roughness such as circular, [Yadav and Bhagoria \(2013b\)](#), rectangular, [Yadav and Bhagoria \(2014a\)](#), equilateral triangular sectioned rib roughened, [Yadav and Bhagoria \(2014b\)](#) and semi-circular, [Yadav and Bhagoria \(2014c\)](#). Results indicated that the heat transfer rate enhancement could be obtained with the consideration of the different rib roughnesses shapes and geometrical parameters such as the relative height e/D and the roughness pitch p/e .

Over years, numerous theoretical, numerical and experimental studies have been performed to evaluate the thermal efficiency of SAH by suggesting different ways of improving the heat transfer rate with lowest pumping power. Very good review papers that deals with the experimental studies of artificially solar air heaters can be found in the literature, i.e., [Hans *et al.* \(2009\)](#), [Bhushan and Singh \(2010\)](#), and [Kumar *et al.* \(2012\)](#). Later, [Sharma *et al.* \(2015\)](#) presented a detailed review of Thermo-hydraulic performance analysis for experimentation studies for artificial roughness rib section of SAH and its effect on the thermo-hydraulic parameter. They reported the increased heat transfer rate with the increase in friction loss when its surface is roughened. Recently, [Kabeel *et al.* \(2017\)](#) presented a detailed review on the diverse types of SAH with the corresponding characteristic to improve the knowledge of the best performing cases

For experimental studies, [Pawar *et al.* \(2013\)](#) conducted experiments study of diamond shaped rib roughness in a SAH duct. They obtained a maximum value of Nusselt number of 84.72 for Reynolds number equal to 14012, and a maximum friction factor value about 0.0194 for Re number of 3010. [Alam *et al.* \(2014\)](#) performed an experimental analysis to calculate the friction losses and heat transfer rate for a SAH duct. The influence of including non-circular holes along V-shaped blockages such as square, and rectangular shapes were considered. The experiments analysis considered different circularity range (1 – 0.6) with

varying the relative blockage height, the pitch ratio, and the angle of attack. Results showed that the maximum increase in Nu number and friction factor could be obtained for a relative pitch of 8 and 4, respectively. The improvement of Nu number has been also obtained for for an angle of attack equal 60° and for a rectangular hole having circularity of 0.69. Experimental and numerical analysis have been performed by [Nine *et al.* \(2014\)](#) to analyse the turbulent flow in rectangular duct having semi-circular ribs. Results showed that the rib height and pitch ratios influenced the heat transfer rate. It is observed that increasing the ratio p/e , the pressure loss decreases for the same Reynolds number. Recently, experimental analysis is carried by [Soi *et al.* \(2018\)](#) to explore the effect of different roughness height and the location of protrusions shapes on the SAH performance. Results showed that the heat transfer rate and the friction factor were respectively 3.9 times and 1.8 times higher in comparison with smooth duct case. Furthermore, the best Nu number was obtained when the relative protrusion location (w/W) is equal to 0.166 and sphericity $\psi=1$. [Bhujade and Shelke \(2018\)](#) performed experimental analysis of three types of turbulators V-shaped, Square shaped and Transverse wedge-shaped turbulator for an absorber plate of SAH system. These three cases were compared with the smooth plate collector case. Results showed that the calculated Nusselt number for these three cases were higher compared to the flat plate case and that the friction factor found to be maximum for the Transverse wedge-shaped turbulator.

For numerical studies, [Yadav and Bhagoria \(2013a\)](#) reported a detailed literature review about the use of CFD tools in the design of SAH. The commercial code ANSYS Fluent have been also used to select the best turbulence model that provides more accurate results compared with the theoretical and experimental data for a conventional Solar Air Heater. Their results indicated that the RNG $k-\epsilon$ model provides better and accurate results in good agreement with the correlations of Dittus-Boelter. [Yadav and Bhagoria \(2014b\)](#) performed numerical investigation to analyse turbulent flow in SAH having equilateral triangular artificially roughened wall for different Re number, and a wide range of the pitch and height ratios. It has been observed that the performance of the roughened SAH depends strongly on the values of Re, roughness height and pitch ratios. The maximum thermal efficiency of the SAH was evaluated and could be obtained at $Re = 15000$, for pitch ratio $p/e=7.14$ and height ratio $e/D=0.042$. For this roughness case, the improvement in the heat transfer was 3.073 times the smooth case. [Gawande *et al.* \(2014\)](#) analysed numerically the performance of SAH with circular transverse ribs in addition to imposed circular vortex generator at the inlet section. For constant roughness height ratio $e/D=0.03$, different value of the pitch ratio varied between $10 \leq p/e \leq 25$ and Re number range between $3800 \leq Re \leq 18000$ have been considered. ANSYS FLUENT code is used and the analysis showed that the imposed circular vortex generator creates more turbulence that contribute in additional enhancement of Nu number with slight

increase in friction factor values. The optimum heat transfer rate was computed to be 2.05 times compared to the duct with smooth absorber plate and 1.06 times compared to the case with ribs alone. Ranjan *et al.* (2015) conducted numerical investigation of SAH having a semi-circular rib roughness. The thermo-hydraulic characteristics were investigated, and results indicated the best obtained thermo-hydraulic characteristic was equal to 1.616 for $e/D=0.06$ and $p/e=7.5$. Gawand *et al.* (2016) performed a numerical simulation of L-shaped rib in solar air channel using ANSYS FLUENT code. Results indicated that the change of Re number and the roughness pitch (p/e) have a substantial effect on the heat transfer rate and the friction coefficient characteristics. Rajneesh Kumar *et al.* (2017a) analysed numerically the performance of a SAH having artificial roughness in the form of elliptical ribs. The effect of the ribs height (e/D), the ribs width (e/w) and ribs pitch (p/e) ratios on the friction factor and heat transfer have been investigated for Re number range between 4000 to 15000. Reynolds-average Navier-Stokes equations (RANS) model have been used for turbulence modelling. They reported that Nu number increases by increasing the ribs height ratio (e/D) and decreases with increasing the ribs width (e/w) and the ribs pitch (p/e) ratios. The maximum Nu and friction factor values could be obtained for $e/w = 0.5$, $e/D = 0.045$ and $p/e = 6$. Further numerical analysis using ANSYS FLUENT code by Rajneesh Kumar *et al.* (2017b) focused on the thermo-hydraulic efficiency of triangular SAH duct with semi-circular artificial roughened ribs. The THPP is evaluated for different ribs sizes (e/D) and arrangements (p/D) for a range of Re number of $4000 \leq Re \leq 24000$. They found that the friction factor decreases when the pitch is increased from 15 to 50 but decreases when the height ratio e/D is increased. The maximum THPP was obtained for $e/D = 0.067$ and for lower value of $p/e = 7.5$.

Later, experiments and numerical simulations were performed by Gawande *et al.* (2016) using chamfered square rib on the heated surface. Investigation were carried out for Re number ranging from 3800 to 18000 for wide range of (p/e) and (e/D). They found that the maximum THPP could be obtained when the chamfer angle equal to 20° . Rajeev Ranjan *et al.* (2017) studied numerically the performance of isosceles right triangle ribs placed on the heated surface of a SAH. They concluded that the maximum THPP performance could be obtained for rib pitch ratio of 5 and rib height ratio 0.045. Menasria and Zedairia (2017) conducted numerical analysis of turbulent convective heat transfer in duct having a rectangular inclined baffle fixed in insulated bottom wall. Different baffle blockage ratios and different baffle-pitch spacing ratios were investigated. The configuration with ($BR=0.7$, $PR=2$ and $Re=5000$) was selected to be the best configuration that provided the highest thermo-hydraulic performance factor. Fawaz *et al.* (2018) analysed numerically the turbulent flow in a square channel having V-baffles mounted in the lower and upper walls with an angle of attack equal to 45° and an in-line arrangement. Re number was varied from

5000 to 25000. They found that the Blockage Ratio BR decreases as the THPP increase.

Recently, theoretical investigation-based energy balance equations of artificial roughened absorber with grooved ribs in solar air collector is performed by Yildirim *et al.* (2018). Results were compared with the case of flat absorber plate investigated the and they compared with the flat plate SAH. Different geometrical roughness parameters including the roughness pitch ratio (RRP), the roughness height ratio (RRH), and the groove locations to pitch ratio (GL/PR) have been tested for Re number range of 3000 to 21,000. Results indicated an increased heat transfer when Re number is increased. Furthermore, the thermal efficiency increased when both; the RRP and the RRH ratios, are increased. However, the maximum thermohydraulic efficiency could be obtained for RRP = 6 and 4 for low and high Re number values. It is shown also that increasing RRH to high values increases the turbulence intensity which provides a higher pressure drop and slightly lower thermohydraulic efficiency. The complicated combination of all above flow and geometrical parameters, motivates the need of further numerical and experimental investigations.

Based on the literature review, it is shown that very little CFD studies on the artificially roughened SAH have been done, more particularly the SAH with triangular ribs having curved top corner. The present work is novel in a way that no such shape of ribs has been previously examined for SAH. The present numerical analysis has been conducted using ANSYS FLUENT 15.0. commercial code. The main objective is to investigate the impact of the roughness height (e/D) and the roughness pitch (p/e) ratios on the Nu number and the friction factor, to determine the best value of parameters that provide the maximum thermal-hydraulic factor.

2. CFD MODELLING

2.1 Geometry Model

The SAH computational domain is a two-dimensional rectangle duct having an aspect ratio width/height $W/H = 5$ with $H = 20$ mm. The duct with the total length L is splitted into three sections, entrance L1, test L2 and exit section L3 as illustrated in Fig. 1. The inlet distance L1 have been chosen to have no influence on the results with the imposed inlet uniform velocity. The computational domain has been created as per the ASHRAE Standard. The ASHRAE Standard 93-2003 recommends a value of $5\sqrt{WH}$ and $2.5\sqrt{WH}$ for the inlet and exit duct length, respectively. This agree well with previous published results of Solar Air Heater (SAH), see Yadav and Bhagoria (2013b, 2014c).

The artificial roughness considered on the absorber surface made of aluminium is a triangular rib having a curved top corner. The present investigation covers a wide range of the roughness height (e/D) and the pitch (p/e) ratios for different Reynolds number of

3800 ≤ Re ≤ 18000. The absorber plate is heated with a constant heat flux q'' = 1000 W/m² and the geometrical and operating conditions are provided in Table 1.

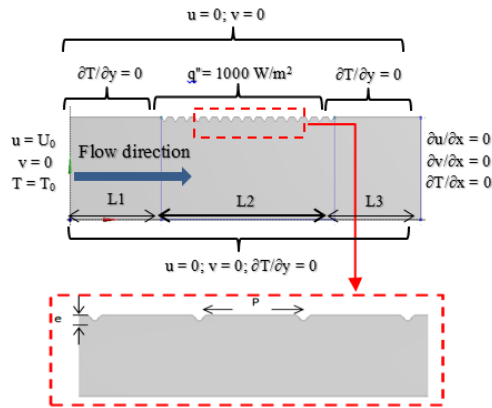


Fig. 1. Schematic of the proposed Solar Air Heater (SAH).

Table 1 Geometrical and operating conditions

Geometrical parameters	Range
Entrance, test and exit section lengths, L1, L2 and L3 (mm)	245, 280 and 115
Hydraulic diameter, D(mm)	33.33
Roughness height, e (mm)	1.4, 1.0 and 0.7
Roughness Pitch, p (mm)	25, 20, 15 and 10
p/e	14.29
e/D	0.042, 0.03, and 0.021 (3 values)

2.2. Grid generation

A non-uniform, structured multi-block grid is considered for the meshing of the present domain as illustrated in Fig. 2. In this case a very refined mesh is used near the duct walls and the transverse roughness surface to accurately resolve the laminar sub-layer, and to obtain an independent grid solution.

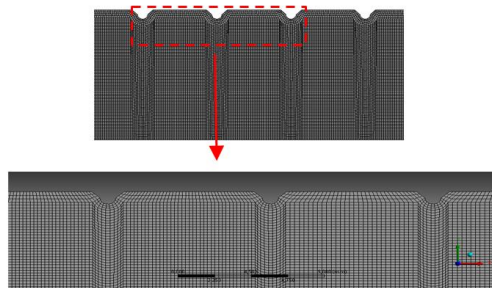


Fig. 2. Schematic of grid systems.

2.3. Governing Equations

The solution of fluid dynamics and heat transfer of air fluid flow in artificially roughened SAH, can be obtained by solving the two-dimensional equations of continuity, momentum and energy given in tensor form, [Menasria and Zedairia \(2017\)](#), as shown below:

Mass conservation:

$$\frac{\partial(\rho u_i)}{\partial x_j} = 0 \quad (1)$$

Momentum:

$$\frac{\partial(\rho u_i u_j)}{\partial x_j} = -\frac{\partial P}{\partial x_i} + \frac{\partial}{\partial x_j} \left[\mu \left(\frac{\partial u_i}{\partial x_j} + \frac{\partial u_j}{\partial x_i} \right) + (-\rho u'_i u'_j) \right] \quad (2)$$

Energy:

$$\frac{\partial}{\partial x_j} (\rho u_i T) = \frac{\partial}{\partial x_j} \left((\Gamma + \Gamma_t) \frac{\partial T}{\partial x_j} \right) \quad (3)$$

Tensor of Reynolds stresses $-\rho u'_i u'_j$ must be modelled to close Eq. (2). The choice of the model is crucial and may affect the accuracy of the results. [Yadav and Bhagoria \(2013a, 2013b\)](#) compared five turbulence models, including Realizable k-ε, RNG k-ε, Standard k-ε, SST k-ω and Standard k-ω models, to study the flow and heat transfer through SAH. Results were compared with experimental data and the RNG k-ε model 'enhanced wall treatment' was reported to be the best model and it is selected for the present study. For the k-ε turbulence model, the viscosity μ_t is described by formulas:

$$\mu_t = \rho C_\mu \frac{k^2}{\varepsilon} \quad (4a)$$

the closure coefficient C_μ :

$$C_\mu = 0.845 \quad (4b)$$

$$\Gamma = \frac{\mu}{Pr} \quad \text{is the thermal diffusivity} \quad (5a)$$

$$\Gamma_t = \frac{\mu_t}{Pr_t} \quad \text{is the turbulent thermal diffusivity} \quad (5b)$$

Dimensionless parameters of the present study are defined as follows:

Reynolds number:

$$Re = \frac{\rho U_0 D_h}{\mu} \quad (6)$$

where D_h is the hydrolic diameter defined as:

$$D_h = \frac{4 \times \text{Section}}{\text{Perimeter}} = D_h = \frac{4 \times (W \times H)}{2 \times (W + H)} \quad (7)$$

The average Nusselt number:

$$Nu = \frac{h D_h}{\lambda} \quad (8)$$

where h represents the heat transfer coefficient which could be obtained directly from the post-processing

of ANSYS Fluent along the heated wall.

The friction factor:

$$f_r = \frac{\left(\frac{\Delta P}{l}\right) D_h}{2\rho U_0^2} \quad (9)$$

where ΔP is the pressure drop along the SAH duct. A higher pumping power is requirement when the pressure drop ΔP is increased. The optimum system is the one that provides a lower pressure drop with higher heat transfer enhancement. So, the use of artificial roughness element for SAH performance enhancement can be defined by a Thermo-Hydraulic Performance Parameter (THPP) reported by [Webb and Eckert \(1972\)](#) which presents the proportion of thermal and fluid dynamic, and is given by the following equation:

$$THPP = \frac{\left(\frac{Nu_r}{Nu_s}\right)}{\left(\frac{f_r}{f_s}\right)^{1/3}} \quad (10)$$

2.4. Boundary Condition:

In the present study, the computational model is consisting of three rectangular sections named, inlet, test and exit sections, respectively. The absorber surface thickness is 0.5 mm and the working fluid, and the absorber plate properties are presented in Table 2. The applied boundary conditions can be defined along each duct section as:

- At the inlet section ($x=0, 0 \leq y \leq H$),

$$u=U_0, v=0 \text{ and } T=T_0 \quad (11)$$

- At the outlet section ($x=L, 0 \leq y \leq H$),

$$\partial u / \partial x = 0; \partial v / \partial x = 0 \text{ and } \partial T / \partial x = 0 \quad (12)$$

- On the top wall ($y = H$)

- On the adiabatic sections $0 \leq x \leq L1$ and $L1 + L2 \leq x \leq L$:

$$u = 0; v = 0 \text{ and } \partial T / \partial y = 0 \quad (13)$$

- On the heated section $L1 \leq x \leq L1+L2$:

$$u = 0; v = 0 \text{ and } q'' = 1000 \text{ (W/m}^2\text{)} \quad (14)$$

- On the bottom wall ($y = 0, 0 \leq x \leq L$),

$$u = 0; v = 0 \text{ and } \partial T / \partial y = 0 \quad (15)$$

Table 2 SAH absorber plate and working fluid properties

Properties	Absorber plate (aluminium)	Working fluid (air)
cp (J/kg k)	871	1006.43
ρ (kg/ m ³)	2719	1.225
λ (w/m k)	202.4	0.0242
μ (N.s/ m ²)	-	1.7894e-05

3. RESULTS AND DISCUSSION

The air (Prandtl number $Pr = 0.7$) enters the duct with a uniform velocity U_0 and an inlet temperature $T_0 = 300$ K. Re number is increased from 3800 to 18000. The absorber plate (test sections) is heated with constant heat flux $q'' = 1000$ (W/m²) and the bottom wall is assumed adiabatic. The exit is invariable pressure boundary with an atmospheric pressure of $1.013 \times \text{Pas}$. Based on the literature study, the RNG k- ϵ model is selected in the present study to calculate the turbulence variables. The convergence criterion considered to guarantee a good accuracy in the computational results is 10^{-6} for the scaled residues of mass, momentum and energy flux. The computations were performed on a laptop, using Intel® core (TM) i5-4210U and the CPU 1.7 GHZ with 8GB RAM (64bits), providing an average computational time of about 35 minutes for each case.

In the present study, numerical investigation on the impact of the pitch (p/e) and the height (e/D) ratios on the thermohydraulic (THPP) performance of SAH is performed for a SAH with triangular artificial roughness having a curved top corner. First, a grid sensitivity test as presented in Table 3 is performed to analyse the independency of the numerical solution and the obtained results are presented in Table 4. To determine the laminar sub-layer, a refine mesh size near the walls is used and results indicates that the friction factor and Nusselt number becomes less than 1% for the mesh 5 when the element size is decreased to 0.3 mm as shown in Table 4. So, the mesh 5 with the total number of elements of 135047 (first element size of 0.3) is used for all computations of the present work.

Table 3 Detail of the tested grids

Mesh	Total number of elements	First element size (mm)
1	48976	0.5
2	59220	0.45
3	75893	0.4
4	115457	0.32
5	135047	0.3
6	150674	0.28

Table 4 Grid sensitivity test

Mesh	Nu	f_t	% Difference Nu	% Difference f_t
1	34.55	0.01558	-	-
2	35.11	0.01586	1.62	1.79
3	35.41	0.01567	0.88	1.29
4	35.68	0.01583	0.46	1.32
5	35.74	0.01583	0.17	0.01
6	35.76	0.01577	0.06	0.41

3.1 Heat Transfer Analysis

3.1.1 Impact of Relative Roughness Pitch (p/e)

Figure 3 shows the impact of Re number on the computed average Nu number for constant value of $e/D=0.042$ and different values of the roughness

pitch ratio (p/e). It is shown that Nu number is increased with increasing Re number due to the change in the flow field and the laminar sub-layer in the turbulent flow region. It is noticed also that Nu number increases with decreasing the ratio p/e and the optimum value of Nu number could be obtained for $p/e = 7.14$. The maximum enhancement in Nu number is about 45.72 % compared to the smooth duct at Re of 18000. The duct with artificial roughness have a higher Nu number compared to the smooth duct, thus the inclusion of artificial roughness elements of different shapes is a key parameter in the design and the improvement of the heat transfer for the SAH.

3.1.2 Impact of Relative Roughness Height (e/D)

Figure 4 shows the effect of Re number on the Nu number for different e/D values and constant value of $p/e=14.29$. It is observed that Nu number increases with increasing both; Re number and the roughness height ratio e/D . The increase of e/D produces more reattachment of the free shear layer and creates local turbulence that provides more air flow mixing with the creation of strong secondary flows. This flow mechanism improves the heat transfer rate.

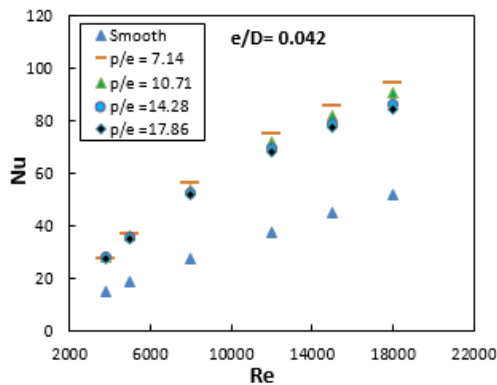


Fig. 3. Nu number variation against Re number for $e/D=0.042$ and for several pitch ratios (p/e).

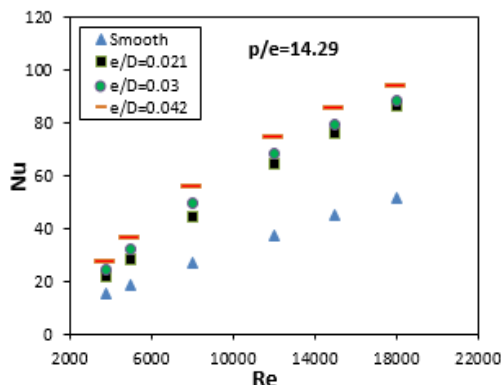


Fig. 4. Nu number variation versus Re number for $p/e=14.29$ and for several height ratios (e/D).

3.2 Friction Factor Calculations

3.2.1 Impact of Roughness Pitch Ratio (p/e)

Figure 5 shows the effect of the pitch ratio (p/e) on

the friction factor for constant value of $e/D=0.042$. Results are presented for several Re number and shows that the friction factor is decreased when Re number is increased. The highest values of the friction factor could be obtained for the minimum value of $p/e = 7.14$. In this case, the surface roughness increases and the resistance to the air flow increases, thus, the friction factor increases because of the separation and reattachment of the laminar sub-layer when Reynolds number is increased.

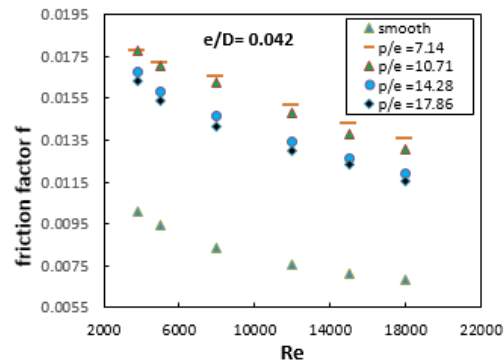


Fig. 5. Friction factor against Re number for $e/D = 0.042$ and for several pitch ratios (p/e).

3.2.2 Impact of Relative Roughness Height (e/D)

Figure 6 shows the variation of the friction factor against Re number for $p/e = 14.29$ and several values of e/D . Results shows that as Re number is increased, the friction factor decreases, and the highest friction factor values are obtained for the greater value $e/D=0.042$ due to the increased wall resistance to the flow.

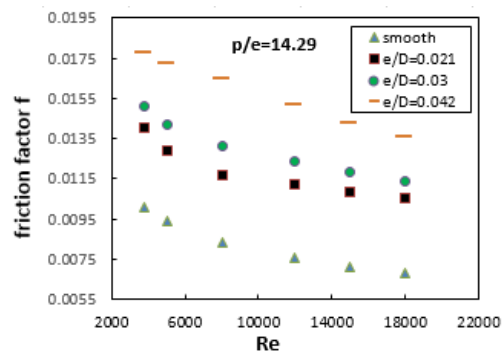


Fig. 6. Friction factor versus Re number for $p/e = 14.29$ and for several height ratios (e/D).

3.3 Thermal Enhancement Factor

The selected roughness ratios e/D and p/e have a significant impact on thermo-hydraulic parameter (THPP) of SAH. The THPP parameter was defined first by Webb and Eckart (1972) and describes the balance between the heat transfer improvement and the friction losses.

The variation of the THPP versus Re number for $e/D=0.042$ and several values of p/e and is presented in Fig. 7 and the variation of the THPP for different values e/D values versus Re number and for p/e of

14.29 is presented in Fig. 8. It is shown that the THPP increases then decreases with increasing Re number. It is shown that the better THPP for a SAH with roughened transverse rib is obtained for $e/D=0.042$.

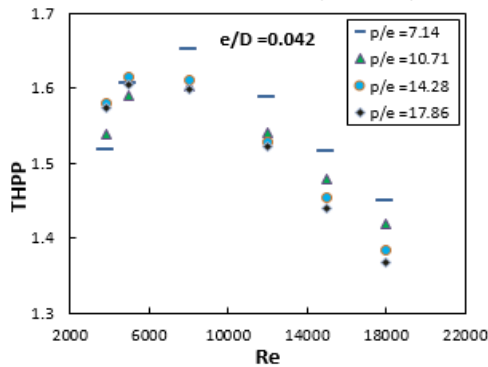


Fig. 7. Variation of THPP versus Re number for $e/D = 0.042$ and for several pitch ratios (p/e).

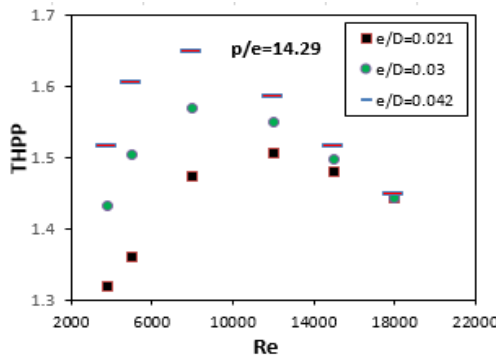


Fig. 8. Variation of THPP versus Re number for $p/e = 14.29$ and for several height ratios (e/D).

As discussed above, the performance of the SAH depends strongly on the presence of the triangular ribs roughness having a curved top corner when compared to the smooth SAH. The reason is that the development of the boundary layer is disturbed by the presence of the artificial roughness and by consequence the turbulent intensity is enhanced due to the enhanced turbulent kinetic energy and the dissipation rate. Figures 9 and 10 present the contour plots of the turbulent kinetic energy k and the turbulent intensity I , respectively, for a fixed value of $e/D=0.042$ and $p/e=7.14$ and for a wide range of Re number $3800 \leq Re \leq 18000$. It is observed that the maximum values of k and I are obtained near the top heated surface and more precisely at the first and second ribs due to the high sheared fluid in this region. It could be observed that the turbulent kinetic energy k is significantly increased when Re number is increased. The turbulent intensity I in Fig. 10 for the case $Re = 8000$ show almost uniform distribution between the downstream ribs with relatively high values. This case matches well

with the best Thermo-Hydraulic Performance Parameter (THPP) obtained in Figs. 7 and 8.

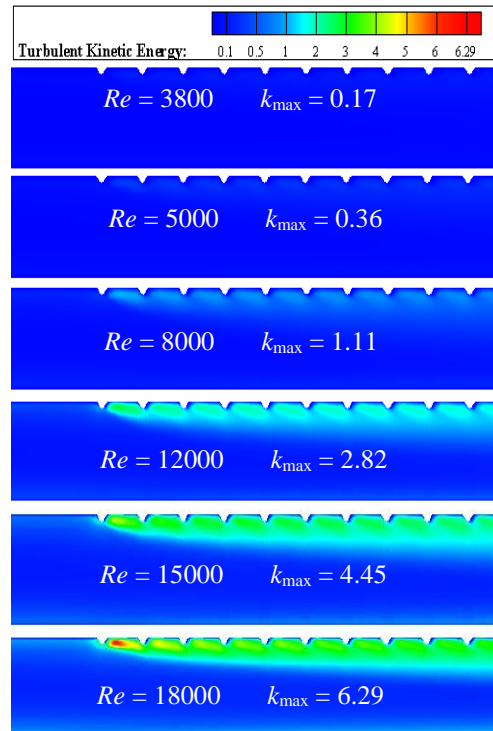


Fig. 9. Turbulent kinetic energy k for $e/D=0.042$ and $p/e=7.14$ for different Re number.

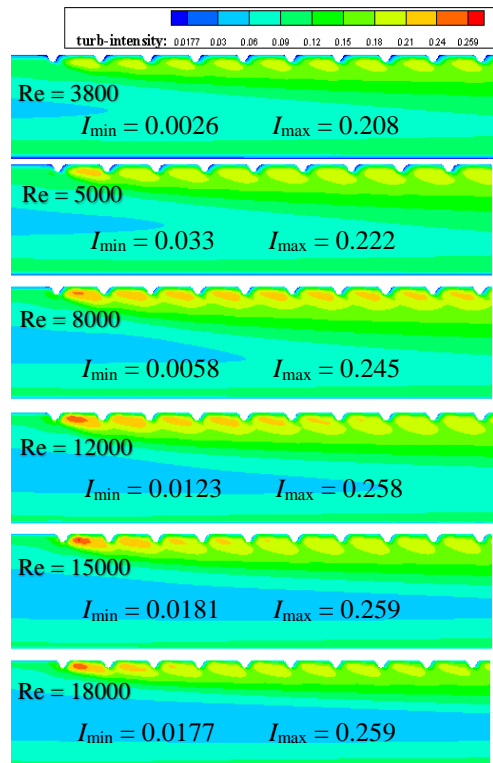


Fig. 10. Turbulent intensity contours for $e/D=0.042$ and $p/e=7.14$, for different Re number.

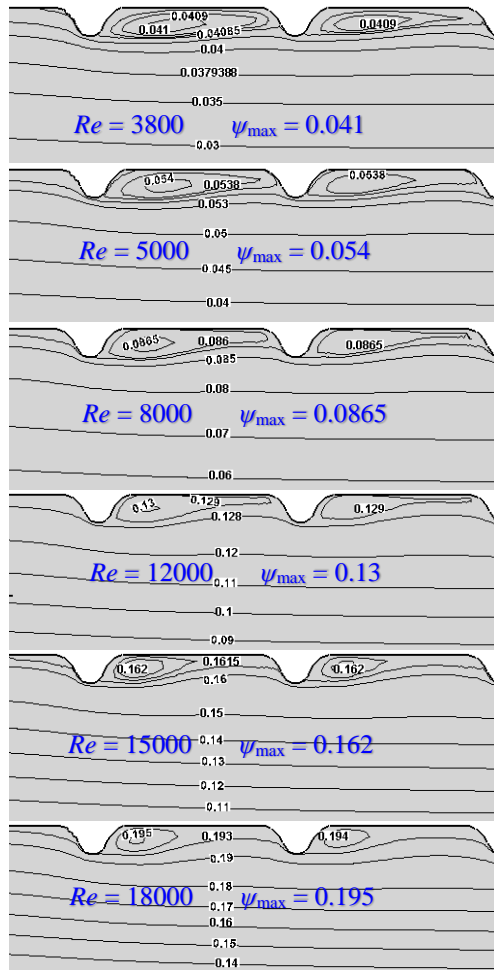


Fig. 11. Streamlines for $p/e=7.14$ and $e/D=0.042$ for different Re number.

Figure 11 shows the streamlines near the two first ribs for fixed value of $e/D=0.042$ and $p/e=7.14$ and for different Re number $3800 \leq Re \leq 18000$. It is observed that stream values are increasing with increasing Re number in which the maximum stream function values varies from $\psi=0.041$ for $Re=3800$ to $\psi=0.195$ for $Re = 18000$. The intensified flow behind the ribs is associated by a decreased vortices sizes when Re number is increased.

Figure 12 shows the contour plots of the static temperature for fixed value of $p/e=7.14$ and $e/D=0.042$ and for different Re number of $3800 \leq Re \leq 18000$. It is observed that the maximum static temperature inside the SAH is decreasing with increasing Re number due to the increased air temperature coming from the inlet section. This provides smaller differences between the bulk and wall temperature and by consequence increasing Nusselt number values.

Figure 13 presents the contour plots of the pressure for $Re=8000$, $p/e=14.28$ and for different values of e/D . It is shown that increasing the roughness relative height (e/D)

leads to an increase in the pressure drop due to the increased resistance to the flowing fluid flow.



Fig. 12. Static temperature contours for $e/D=.042$ and $p/e=7.14$ for different Re number.

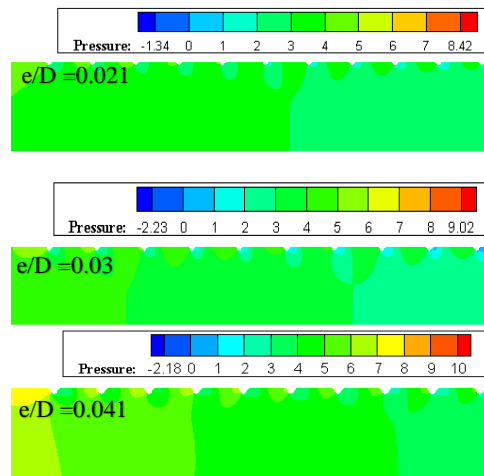


Fig. 13. Pressure contours for $Re = 8000$, $p/e=14.29$ and different height ratios (e/D).

3.4 Validation of the Model

Results of the present computational domain are compared with the experimental and numerical results produced in Figs. 14 and 15, respectively. Further comparison is conducted with the numerical results of [Yadav and Bhagoria \(2014a\)](#) for the case of semi-circular transverse rib roughness as introduced in Fig. 14.

Results show the comparison of the computed friction factor with the experimental data of [Nine *et al.* \(2014\)](#), and the numerical results of [Yadav and Bhagoria \(2014a\)](#). Figure 15 show the comparison between the present results and those of [Yadav and](#)

Bhagoria (2014a) for the variation of Nu number against Re number. In general, a good agreement with Yadav's numerical results is obtained and agree well with the experimental results of Nine *et al.* (2014).

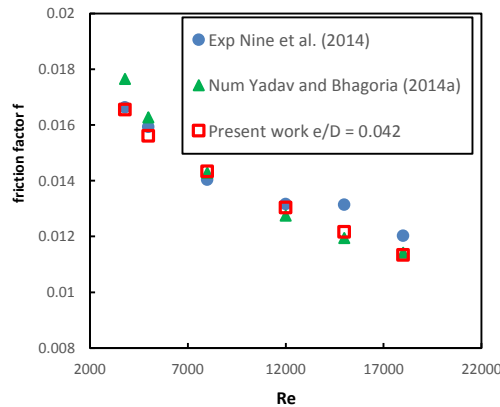


Fig. 14. Friction factor of present CFD with results of Nine *et al.* (2014) and Yadav and Bhagoria (2014a).

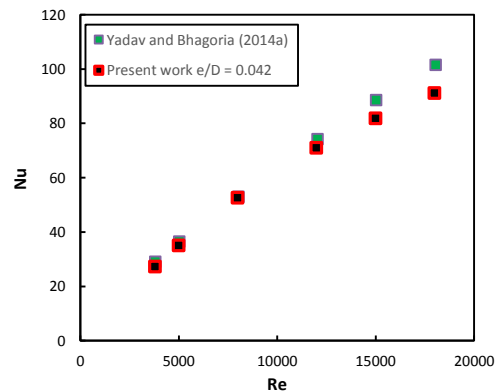


Fig. 15. Validation the Nu number of numerical result with Yadav and Bhagoria (2014a).

5. CONCLUSIONS

In the present numerical investigation, a solar air heater SAH with a triangular artificial roughness having a curved top corner is considered. A wide range of Re number and protrusion parameters are considered. From the provided results and the analysis of the flow and the heat transfer characteristics, the following conclusion can be drawn:

- Nu number increases with increasing Re number. However, the friction factor decreases with increasing Re number for all combination of e/D ratio.
- Nu number increases with increasing p/e ratio for a fixed e/D ratio.
- Nu number increases with increasing the e/D ratio for a fixed p/e ratio.
- Friction factor increases with decreasing the p/e ratio for a fixed e/D ratio.
- It is found that the optimum value of THPP for the present investigated SAH with transverse rib roughness could be obtained for a value of p/e = 7.14 and a fixed value of e/D = 0.042.

REFERENCES

- Alam, T., R. P. Saini and J. S. Saini (2014). Effect of circularity of perforation holes in V-shaped blockages on heat transfer and friction characteristics of rectangular solar air heater duct. *Energy Conversion and Management* 86, 952–963.
- ASHRAE Standard 93, (2003), Method of Testing to Determine the Thermal Performance of Solar Collectors. American Society of Heating, Refrigeration and Air Conditioning Engineers, Atlanta, GA30329.
- Bhujade, S. D. and R. S. Shelke (2018). Performance of Solar Air Heater System Using Different Shapes of Turbulators on the Absorber Plate. *International Journal of Engineering and Creative Science* 1 (1) 31–35.
- Bhushan B. and R. Singh (2010). A review on methodology of artificial roughness used in duct of solar air heaters. *Energy* 35 (1) 202–212.
- Fawaz, H. E., M. T. S. Badawy, M. F. Abd Rabbo and A. Elfeky (2018). Numerical investigation of fully developed periodic turbulent flow in a square channel fitted with 45° in-line V-baffle turbulators pointing upstream, *Alexandria Engineering Journal*, 57 (2) 633–642.
- Gawande, V. B., A. S. Dhoble and D. B. Zodpe (2014). CFD analysis to study effect of circular vortex generator placed in inlet section to investigate heat transfer aspects of solar air heater. *The Scientific World Journal* 2014, 11.
- Gawande, V. B., A. S. Dhoble, D. B. Zodpe, and S. Chamoli (2016). Experimental and CFD-based thermal performance prediction of solar air heater provided with right-angle triangular rib as artificial roughness. *Journal of the Brazilian Society of Mechanical Sciences and Engineering* 38 (2) 551–579.
- Hans, V. S. Saini, R. P. and Saini, J. S. (2009) Performance of artificially roughened solar air heaters—a review, *Renewable and Sustainable Energy Reviews* 13(8), 1854–1869.
- Jaurker, A. R., J. S. Saini and B. K. Gandhi (2006). Heat transfer and friction characteristics of rectangular solar air heater duct using rib-grooved artificial roughness. *Solar Energy* 80 (8) 895–907.
- Kabeel, A. E., M. H. Hamed, Z. M. Omara and A. W. Kandeal (2017). Solar air heaters: Design configurations, improvement methods and applications – A detailed review. *Renewable & Sustainable Energy Reviews* 70, 1189–1206.
- Kumar, A., R. P. Saini and J. S. Saini (2012). Heat and fluid flow characteristics of roughened solar air heater ducts—a review. *Renewable*

- Energy* 47, 77–94.
- Kumar, R., V. Geol, and A. Kumar, (2017a). A parametric study of the 2D model of solar air heater with elliptical rib roughness using CFD. *Journal of Mechanical Science and Technology* 31 (2) 959–964.
- Kumar, R., Kumar, A. and Varun, (2017b) "Computational fluid dynamics based study for analyzing heat transfer and friction factor in semi-circular rib-roughened equilateral triangular duct", *International Journal of Numerical Methods for Heat & Fluid Flow*, 27 (4), 941-957.
- Menasria F. and M. Zedairia (2017). Numerical study of thermohydraulic performance of solar air heater duct equipped with novel continuous rectangular baffles with high aspect ratio. *Energy* 133, 593–608.
- Nine, J., G. H. Lee, H. S. Chung, M. Ji and H. Jeong (2014). Turbulence and pressure drop behaviors around semicircular ribs in a rectangular channel. *Thermal Science* 18 (2) 419–430.
- Pawar, S. S., D. A. Hindolia and J. L. Bhagoria (2013). Experimental study of Nusselt number and Friction factor in solar air heater duct with Diamond shaped rib roughness on absorber plate. *American Journal of Engineering Research* 2 (6) 60–68.
- Ranjan, R., M. K. Paswan and N. Prasad (2015). CFD Investigation of Artificially Roughened Solar Air Heater for Performance Enhancement. *International Advanced Research Journal in Science, Engineering and Technology* 2 (9) 59–64.
- Ranjan, R., M. K. Paswan and N. Prasad (2017). CFD based analysis of a solar air heater having isosceles right triangle rib roughness on the absorber plate. *International Energy Journal* 17 (2) 57–74.
- Sharma, S. K. and V. R. Kalamkar (2015). Thermo-hydraulic performance analysis of solar air heaters having artificial roughness-A review. *Renewable & Sustainable Energy Reviews* 41, 413–435.
- Soi, A., R. Singh and B. Bhushan (2018). Heat transfer and friction characteristics of solar air heater duct having protruded roughness geometry on absorber plate. *Experimental Heat Transfer* 31 (6) 571–585.
- Webb, R. L. and E. R. G. Eckert (1972). Application of rough surfaces to heat exchanger design. *International Journal of Heat and Mass Transfer* 15 (9) 1647–1658.
- Yadav, A. S. (2015). CFD investigation of effect of relative roughness height on Nusselt number and friction factor in an artificially roughened solar air heater. *Journal of the Chinese Institute of Engineers* 38 (4) 494–502.
- Yadav A. S. and J. L. Bhagoria (2013a). Heat transfer and fluid flow analysis of solar air heater: A review of CFD approach. *Renewable & Sustainable Energy Reviews* 23, 60–79.
- Yadav A. S. and J. L. Bhagoria (2013b). A CFD (computational fluid dynamics) based heat transfer and fluid flow analysis of a solar air heater provided with circular transverse wire rib roughness on the absorber plate. *Energy* 55, 1127–1142.
- Yadav A. S. and J. L. Bhagoria (2014a). A numerical investigation of turbulent flows through an artificially roughened solar air heater. *Numerical Heat Transfer Part A* 65 (7) 679 – 698.
- Yadav A. S. and J. L. Bhagoria (2014b). A CFD based thermo-hydraulic performance analysis of an artificially roughened solar air heater having equilateral triangular sectioned rib roughness on the absorber plate. *International Journal of Heat and Mass Transfer* 70, 1016–1039.
- Yadav A. S. and J. L. Bhagoria (2014c). A numerical investigation of square sectioned transverse rib roughened solar air heater. *International Journal of Thermal Sciences*, 79, 111–131.
- Yıldırım, C. and N. F. Tümen Özdil (2018). Theoretical investigation of a solar air heater roughened by ribs. *Journal of Thermal Engineering* 4(1), 1702–1712.